Search-Based Adversarial Estimates for Improving Sample Efficiency in Off-Policy Reinforcement Learning

Federico Malato [1] **Ville Hautamäki** [1]

Abstract

Sample inefficiency is a long-lasting challenge in deep reinforcement learning (DRL). Despite dramatic improvements have been made, the problem is far from being solved and is especially challenging in environments with sparse or delayed rewards. In our work, we propose to use Adversarial Estimates as a new, simple and efficient approach to mitigate this problem for a class of feedback-based DRL algorithms. Our approach leverages latent similarity search from a small set of human-collected trajectories to boost learning, using only five minutes of human-recorded experience. The results of our study show algorithms trained with Adversarial Estimates converge faster than their original version. Moreover, we discuss how our approach could enable learning in feedback-based algorithms in extreme scenarios with very sparse rewards.

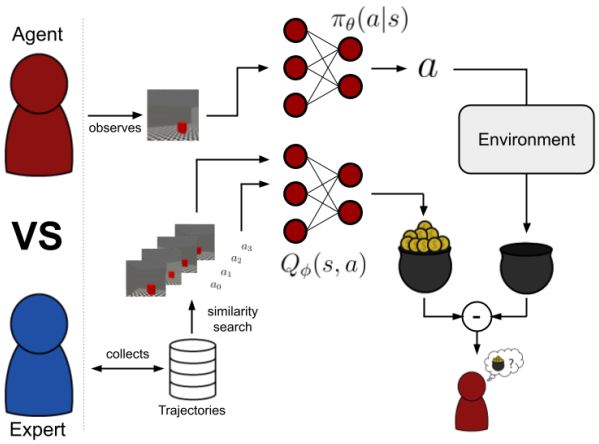

Figure 1. A schematic illustration of our proposed method, Adversarial Estimates. The agent sees the expert as an adversary. At each timestep, the reward obtained by the agent is compared to the estimated reward obtained by the expert in similar situations, retrieved from a set of expert trajectories. This feedback is then used to guide training.

1. Introduction

Sample inefficiency is a long-lasting challenge in *deep reinforcement learning* (DRL) affecting all well-known algorithms, such as Deep-Q-Network (DQN) (Mnih et al., 2015), Deep Deterministic Policy Gradient (DDPG) (Lillicrap et al., 2019) and Soft Actor Critic (SAC) (Haarnoja et al., 2018). The problem relates to the high number of transitions needed to learn an optimal policy (Sutton & Barto, 2018). Sample inefficiency has several causes, ranging from a high-dimensional observation or action spaces (Mnih et al., 2015), to an ineffective exploration strategy (Bellemare et al., 2016), or even an ill-designed reward signal (Rengarajan et al., 2022). In general, a good reward signal should be mathematically well-defined and encapsulate the learning objective perfectly (Sutton & Barto, 2018). Unfortunately, specifying a reward signal with these properties is generally a non-trivial task, and in some cases it might not be possible at all (Shakya et al., 2023; Zare et al., 2023; Rengarajan et al., 2022). It is possible to address this shortcoming by defining a *sparse* reward, that is, assigning a positive constant value only to certain transitions. As an example, consider the case of a robot moving in a room, whose objective is to move to a certain goal, given an initial position. If the distance between the robot and the goal position can be computed, then the inverse of that distance could be used as a good, dense reward signal; if this is not possible, though, a good solution would be to assign a value of 1 upon reaching the goal, and 0 otherwise. The latter case represents an example of sparse reward. Additionally, such reward is also *delayed*, as the robot will not observe it until the end of an episode.

Using sparse and delayed reward simplifies the task of specifying the goal of a task; unfortunately, the sporadic feedback turns the task into an harder one to learn. In particular, a sparse reward signal could prevent an agent from collecting meaningful experience, thus delaying or preventing learning (Lillicrap et al., 2019; Rengarajan et al., 2022).

[1]School of Computing, University of Eastern Finland, Joensuu, Finland. Correspondence to: Federico Malato <federico.malato@uef.fi>.

Proceedings of the 42^{nd} International Conference on Machine Learning, Vancouver, Canada. PMLR 267, 2025.

Table 1. A summary of the most relevant previous research used as inspiration for our work.

Paper	Description	Algorithms	Assumes expert optimality	Main features
DQN/DDPG from Demonstrations (DQfD)/(DDPGfD) (Hester et al., 2017)/ (Vecerik et al., 2018)	Loads human-collected experience in replay buffer and adapts DQN/DDPG objective	DQN/ DDPG	Yes	Pre-training; Mixture random sampling; Distribution-based update
Reincarnating RL (Agarwal et al., 2022)	Uses previous experience from policy or human expert as teacher in a DAgger-like approach	Off-policy algorithms	**No**	Pre-training; Mixture random sampling; Distribution-based update
Learning Online from Guidance Offline (LOGO) (Rengarajan et al., 2022)	Entropy-based loss regularization to learn from human-collected trajectories	TRPO	**No**	Mixture random sampling; Distribution-based update
Advantage Weighted Actor-Critic (AWAC) (Nair et al., 2021)	Defines closed-form solution for KL-bounded update based on expert policy	Off-policy algorithms	Yes	Pre-training; Mixture random sampling; Distribution-based update
Adversarial Estimates (Ours)	Uses search on human-collected experience to boost Q-values convergence	Off-policy algorithms	**No**	Search-based sampling

Similarly, an agent acting to solve a task with delayed rewards might not experience positive reinforcement very often, increasing the number of transitions sampled to converge (Andrychowicz et al., 2018). Despite vast efforts in this field and many proposed solutions, the problem of mitigating sample inefficiency for sparse or delayed reward tasks is still an open problem (Shakya et al., 2023).

Previous research can be divided into three categories, depending on the approach used to address the problem of sample efficiency. The first category proposes to include offline data in the replay buffer of an off-policy algorithm at the beginning of training, and to adapt the learning objective accordingly. This line of research is used in *Deep-Q-Learning from Demonstrations* (DQfD) (Hester et al., 2017) and *Deep Deterministic Policy Gradients from Demonstrations* (DDPGfD) (Vecerik et al., 2018). The second category proposes to add a pre-training phase using only human expert data, and subsequently fine-tuning the policy online using a distribution-based penalty term to the loss. Examples of this approach are (Schmitt et al., 2018), QDagger (Agarwal et al., 2022) and *Learning Online from Guidance Offline* (LOGO) (Rengarajan et al., 2022). Finally, a third category combines ideas from both groups, such as *Advantage Weighted Actor Critic* (AWAC) (Nair et al., 2021). For their approach, the authors preload an offline dataset in the replay buffer and use it for pre-training their policy. Then, they fine-tune their policy using a loss derived from a KL-constrained optimization problem.

In our work, we propose to detach from three key aspects of previous methods: the need for pre-training, the distribution-based regularization, and the narrow application to algorithms. Firstly, although pre-training perfectly serves its purpose of transferring knowledge between policies (Agarwal et al., 2022), we deem this step unnecessarily long for standard policy training. Additionally, such phase might rely on high-quality data from an optimal or near-optimal expert, which might be impractical for complex tasks. In second instance, relying on a distribution-based regularizer biases the policy to follow the expert. If the expert is considered optimal (Hester et al., 2017; Vecerik et al., 2018; Nair et al., 2021), the trained policy will at most match those performance. This is a problem when the expert is suboptimal, hence binding the learned policy to be suboptimal as well (see Figure 2). A solution to this is gradually detaching from the expert policy using a decaying hyperparameter (Rengarajan et al., 2022). While this allows for

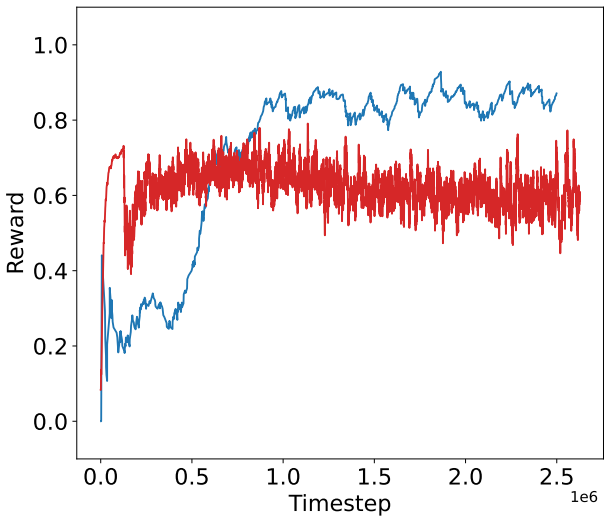

Figure 2. An example of policy converging to a local minimum when the expert optimality assumption does not hold. With respect to the baseline (blue), the kickstarted policy π_θ (orange) learns much faster at the beginning of training. Still, performance saturates due to the joint effect of expert not being optimal and the distribution-based constraint.

an improvement over the expert, it usually comes with a degradation in performance, as the sudden drop of the red line in Figure 2 shows. Finally, previous approaches such as AWAC show that it is possible to find a broadly applicable update rule. As such, although previous work (Hester et al., 2017; Vecerik et al., 2018; Rengarajan et al., 2022) shows that tweaking a specific algorithm leads to an improvement, we consider these results to have limited application.

Mainly inspired by QDagger and AWAC, and leveraging *Bayesian online adaptation* (BOA) (Malato & Hautamäki, 2024), we propose to improve sample efficiency in delayed reward environments by combining standard DRL and similarity search (in the form of *online adaptation*) on a small pool of human-collected trajectories. **Our contributions are three-fold**: first, we derive a general solution for the loss penalization approach, which allows us to overcome limitations arising from the expert optimality assumption (Torabi et al., 2018); second, we remove the need for pre-training, while keeping the broad applicability of such method to any off-policy RL algorithm; third, we reduce the amount of data needed, and remove the need for a pre-trained policy, by using only five minutes of collected experience from a human expert. Additionally, in Section 7 we discuss the possibility of further extending our idea to on-policy algorithms, highlighting the broad applicability of our approach.

2. Related Work

A summary of the information discussed in this Section is reported in Table 1. The Table reports a list of approaches that are closely related to our proposal. For each source, we report a brief description of its main points, a list of compatible DRL algorithms, whether the optimality of expert is assumed, and a short overview of its main features.

In detail, *Deep-Q-Learning from Demonstrations* (DQfD) (Hester et al., 2017) and *DDPG from Demonstrations* (DDPGfD) (Vecerik et al., 2018) leverage human-collected trajectories and add a supervised margin loss term, a 1-step and an n-step double Q-Learning terms, and an L2 regularization term to the loss. Each term addresses and corrects a specific failure case, such as a non-representative dataset for the margin loss and stability of training for the double Q-learning terms.

In (Schmitt et al., 2018), authors collect experience from previously trained agents to train new ones. This approach assumes that an optimal policy exists and can be trained for the task at hand. As such, we point out that such method would be best applicable to e.g. transfer learning from simulations to autonomous agents such as robots acting in the real world.

For *QDagger* (Agarwal et al., 2022), authors suggest that suboptimal data coming from either pre-trained policies or human experts could be used to train a student network. Their method is based on adding an entropy-based penalty term to the loss function. Additionally, QDagger requires an offline pre-training phase, which we avoid in our proposal.

In (Rengarajan et al., 2022), the authors propose a new framework, *Learning Online from Guidance Offline* (LOGO), and derive a penalty term based on KL-divergence for *Trusted Region Policy Optimization* (TRPO) (Schulman et al., 2017a). More specifically, authors propose to alternate between a policy improvement and a policy guidance step. During policy improvement, the agent is trained using TRPO. Then, an additional step to guide the policy towards the expert *while remaining in the truster region* is performed. We point out that the algorithm is specifically tailored on one learning algorithm, TRPO, whereas we propose a generic method that is widely applicable; additionally, LOGO performs two gradient steps for each update, effectively increasing training time. Finally, in the case of partial observability authors propose to train an additional critic for the expert and a discriminator to estimate the current policy performance w.r.t. the expert. We highlight that training additional models might introduce instabilities and propagate errors that lead to catastrophic results.

Similarly, *Advantage Weighted Actor Critic* (AWAC) (Nair et al., 2021) derives a closed-form update to train a policy on a mixture of offline and online data, starting from a

constrained optimization problem based on KL-divergence between a policy and an expert. Although being tested only on SAC, the method is applicable to virtually any off-policy algorithm. AWAC features an offline pre-training step and initializes the replay buffer with human expert trajectories at the beginning of the online training phase, similar to DQfD and DDPGfD.

3. Preliminaries

In RL and DRL, our aim is to train a policy $\pi_\theta : S \to A$ parameterized by a set of parameters θ to select actions that, at any timestep t, maximize the expected sum of discounted future rewards

$$\mathbb{E}[\sum_{\tau=t}^{\infty} \gamma^{\tau-t} r_\tau]. \tag{1}$$

3.1. Markov decision process

We model our problem as a *Markov decision process* (MDP). Formally, the problem is defined as a 5-tuple (S, A, T, R, γ), where we denote $S \subseteq \mathbb{R}^d$ as the d-dimensional state space, A as a continuous or discrete action space, $T : S \times A \to S$ the (unknown) transition dynamics, $R : S \times A \to \mathbb{R}$ a reward function, and $\gamma \in [0, 1)$ as the discount factor.

Additionally, our image-based experiments are modeled on a *partially observable Markov decision process* (POMDP). Such problems represent a generalization of MDPs where the full state of the environment is not observable by the agent. Formally, the problem is defined as a 7-tuple $(S, A, T, R, \Omega, O, \gamma)$ where, other than the previously defined S, A, T, and R, we introduce a set of (partial) observations $\Omega \subseteq \mathbb{R}^d$, and a function $O : S \times A \to \Omega$ mapping the probability of observing $o \in \Omega$, given a certain state $s \in S$ and an action $a \in A$.

3.2. Clipped Double-Q-Learning

Clipped Double-Q-Learning (cDQL) (Fujimoto et al., 2018) is an off-policy value function algorithm for DRL based on the concept of temporal difference (TD) error. The algorithm is a tweaked version of DQN that improves stability during training. At each timestep t, a policy π_θ greedily selects an action a_t following

$$a_t = \underset{a \in A}{\operatorname{argmax}}\, Q^t(s_t, a) \tag{2}$$

where

$$Q^t(s_t, a) = \mathbb{E}[R_t | s_t, a, \pi_\theta], R_t = \sum_{\tau=t}^{\infty} \gamma^{\tau-t} r_\tau. \tag{3}$$

Subsequently, the algorithm updates its Q-values using

$$Q^{t+1}(s_{t+1}, a) = \mathbb{E}[r_t + \gamma \max_{a' \in A} Q^t(s_t, a) | s_{t+1}, a]. \tag{4}$$

Differently from the standard DQN, cDQL uses two twin neural networks to estimate the policy: one is updated with gradient methods; the second one, called the *target network* is updated with lower frequency by soft-updating the weights of the policy network. This is done to avoid overshooting. In particular, cDQL bounds the Q-values by computing the current estimate y_t as

$$y_t = r_t + \gamma \min(Q^t_\theta(s_t, a_t), Q^t_\phi(s_t, a_t)), \tag{5}$$

where ϕ are the parameters of the target network. cDQL minimizes

$$\mathcal{L}(\theta) = \mathbb{E}_t[(y_t - Q^{t+1}_\theta(s_{t+1}, a_{t+1}))^2]. \tag{6}$$

3.3. Advantage Weighted Actor Critic

Given a guidance policy π_β, AWAC aims at efficiently finding an optimal policy π^* by leveraging a dataset $\mathcal{D}$ collected from π_β. In particular, a parameterized policy π_θ is trained following

$$\theta_{k+1} = \underset{\theta}{\operatorname{argmax}}\, \mathbb{E}_{s,a \sim \mathcal{D}}[\log \pi_\theta(a|s) \exp \frac{1}{\lambda} A^{\pi_k}(s, a)] \tag{7}$$

which is equivalent to adding a weighted regularization term $D_{\mathrm{KL}}(\pi_\theta || \pi_\beta)$ to the off-policy loss (Equations 6 and **??**).

3.4. Bayesian online adaptation

BOA uses Bayesian statistics to update the belief of a DRL agent, given a parameterized policy π_θ, a prior distribution $\pi_\theta(a_t^{(\theta)}|s_t)$ and an expert policy π_E. By modeling the prior as

$$\pi_\theta(a_t^{(\theta)}|s_t) \sim \mathrm{Dirichlet}(K, \alpha_{\mathrm{prior}}) \tag{8}$$

with $K = |A|$, $\alpha_{\mathrm{prior},i} = \pi_\theta(a_t^{(\theta)} = i|s_t)$ and we leverage Bayesian statistics to compute the posterior

$$\pi_\theta(a_t^{(\theta)}|a_t^{(E)}, s_t) \propto \pi_E(a_t^{(E)}|a_t^{(\theta)}, s_t)\pi_\theta(a_t^{(\theta)}|s_t) \tag{9}$$

which is still a Dirichlet with K components and $\alpha_{\mathrm{posterior}} = \alpha_{\mathrm{prior}} + c_t$, where c_t is a vector storing the number of occurrences of each action sampled from π_E. In substance, we can update the belief of a network following the "suggestions" of an arbitrary expert policy. In (Malato & Hautamäki, 2024), π_E is chosen to be a simple search-based policy that, at each timestep t, retrieves the k-most similar stored latents to the current state s_t from a pre-encoded, small demonstration dataset.

4. Adversarial Estimates

As highlighted in Table 1, previous research incorporates offline experience, either sampled from a previously trained policy or collected by human contractors, to improve the

quality of experience collected by the agent during training. Notably, all methods explicitly use an offline dataset along with the experience in the replay buffer, either mixing the two sets ((Hester et al., 2017; Vecerik et al., 2018)), or sampling a mixture of experiences ((Nair et al., 2021; Agarwal et al., 2022; Rengarajan et al., 2022)). Motivated by these attempts, we propose an alternative view to the problem of improving sample efficiency.

Differently from previous approaches, we focus on leveraging human-collected experience to boost the convergence rate of Q-values using *Adversarial Estimates*. Loosely inspired by sealed bid auction games, we suppose a competitive scenario in which two players, A and B, are bidding without knowing the opponent strategy or utility function. Intuitively, if player A knows the utility function of player B, they might adjust their beliefs and, as a consequence, their bidding *before* the bidding itself.

Similarly, we propose an adversarial scenario for single agent RL, in which the agent π_θ plays to improve over an expert π_E. π_θ does not know the rewards obtained by π_E. Still, it can *estimate* such returns, by assuming that both players are following the same objective.

Intuitively, we want π_θ to pursue close or winning scenarios over π_E; on the contrary, we want to refute situations where the performance gap is unfavorable for the agent. As such, we propose an adversarial estimate of the form

$$Z_t(s,a) = E_{(s',a')\sim\mathcal{D}}[Q^t_\phi(s',a')] - R_t(s,a), \tag{10}$$

where Q_ϕ denotes the target network, $(s',a') \sim \mathcal{D}$ are state-action pairs extracted from the expert dataset $\mathcal{D}$ using similarity search, and $R_t(s,a)$ is the *actual* reward observed at timestep t.

In our formulation, we over-estimate the rewards obtained by the opponent π_E using search (Malato & Hautamäki, 2024), and compare them to the actual rewards obtained by the policy π_θ. The effect of this choice is two-fold. First, we match the penalty terms proposed in previous work, since $Z_t(s,a) \to 0$ as $R_t(s,a) \to E_{(s',a')\sim\mathcal{D}}[Q^t_\phi(s',a')]$, that is, when the agent matches the *expected, over-estimated performance* of the expert. Notably, our update does not bound π_θ to lie in the vicinity of π_E. Secondly, we ensure faster convergence of the Q-values by sampling multiple *similar* transitions from $\mathcal{D}$ and averaging their estimated returns. In practice, this creates a "more realistic expectation" on state s, which is then implicitly propagated in the loss through $Z_t(s,a)$.

4.1. Mathematical derivation

The first part of our derivation follows (Nair et al., 2021). We aim at solving a constrained optimization problem of the form

$$\pi_{k+1} = \underset{\pi\in\Pi}{\operatorname{argmax}}\, \mathbb{E}_{a\sim\pi(\cdot|s)}[R^{\pi_k}(s,a)] \tag{11}$$

$$\text{s.t.} \quad D_{\mathrm{KL}}(\pi(\cdot|s)||\pi_\beta(\cdot|s)) \le \epsilon, \tag{12}$$

where $\pi_\beta(\cdot|s)$ is an expert policy. Note that, differently from AWAC, we formulate the problem in term of maximization of a reward function $R^{\pi_k}(s,a)$ following a policy π_k. As such, our formulation, in principle, covers any algorithm that aims at maximizing a reward.

By enforcing the KKT conditions, we derive a lagrangian solution for our problem

$$\begin{aligned}\mathcal{L}(\pi,\lambda) = \mathbb{E}_{a\sim\pi(\cdot|s)}[R^{\pi_k}(s,a)] + \\ +\lambda(\epsilon - D_{\mathrm{KL}}(\pi(\cdot|s)||\pi_\beta(\cdot|s))),\end{aligned} \tag{13}$$

which is equivalent to the dual problem

$$\min_{\lambda\ge 0}\max_{\pi\in\Pi} \mathcal{L}(\pi,\lambda). \tag{14}$$

In our formulation, λ regulates the interaction between the two terms in $\mathcal{L}(\pi,\lambda)$. More specifically, it expresses the importance of being close to the expert policy π_β. As such, we relax our problem and consider λ a hyperparameter. After dropping the constant term $\lambda\epsilon$, we are therefore left with

$$\max_{\pi\in\Pi} \mathbb{E}_{a\sim\pi(\cdot|s)}[R^{\pi_k}(s,a)] - \lambda D_{\mathrm{KL}}(\pi(\cdot|s)||\pi_\beta(\cdot|s))), \tag{15}$$

which is equivalent to minimizing

$$\mathcal{L}(\theta) = \mathbb{E}_{a\sim\pi_\theta(\cdot|s)}[R^{\pi_k}(s,a)] + \lambda D_{KL}(\pi_\theta(\cdot|s)||\pi_\beta(\cdot|s))). \tag{16}$$

Following (Nair et al., 2021), we notice that π_θ can be projected in a parameterized policy space using either direction of the KL divergence. Specifically, by choosing the reverse formulation we can estimate it by simply sampling transitions from π_β. In our specific scenario, we choose $\pi_\beta = \pi_E$, that is, the expert policy used in (Malato & Hautamäki, 2024). That is, at each timestep we can retrieve the k-most relevant transitions from our dataset $\mathcal{D}$ and use them as minibatch to enforce the KL constraint.

For the second part of our derivation, we aim at demonstrating the validity of our update in place of the KL constraint. In particular, we want to prove that using $Z_t(s,a)$ (Equation 10) instead of the KL term leads to a relaxation of the optimization problem posed in Equation 16.

First, we need to prove that the two updates share the same objective. To this end, we remove the optimality assumption

of π_E. That is, we consider that there will exist at least one policy π in the space of policies Π such that

$$\mathbb{E}_{(s',a')\sim\pi}[R(s',a')] \geq \mathbb{E}_{(s',a')\sim\pi_E}[R(s',a')]. \quad (17)$$

In this case, we say that $\pi \in \Pi_{\geq E}$ by defining

$$\Pi_{\geq E} := \{\pi | \mathbb{E}_{(s',a')\sim\pi}[R(s',a')] \geq \mathbb{E}_{(s',a')\sim\pi_E}[R(s',a')]\}. \quad (18)$$

By definition, $\pi_E \in \Pi_{\geq E}$. We now consider that

$$D_{\mathrm{KL}}(\pi_\theta || \pi_E) \xrightarrow{\pi_\theta \to \pi_E} 0, \quad (19)$$

that is, the KL divergence will reach its minimum as the policy converges towards the expert. Similarly,

$$Z_t(s,a) \xrightarrow{\pi_\theta \to \pi} 0, \pi \in \Pi_{\geq E}. \quad (20)$$

By imposing $\pi = \pi_E$, we find that $Z_t(s,a)$ behaves numerically as $D_{\mathrm{KL}}(\pi_\theta || \pi_E)$. We can therefore re-write our loss as

$$\mathcal{L}_{\mathrm{AE}}(\theta) = \mathbb{E}_{a\sim\pi_\theta(\cdot|s)}[R^{\pi_k}(s,a)] + \lambda Z_t(s,a). \quad (21)$$

This objective admits all the solutions of Equation 16, with the (possible) addition of new, *at least equally performing* ones. That is, $Z_t(s,a)$ relaxes this minimization problem.

Intuitively, the KL constraint limits π_θ to be close to π_E. We argue that such limitation is desirable only on the assumption that π_E is effectively an optimal policy, or that it is represented as such from the data in $\mathcal{D}$ (Zare et al., 2023). Consistently with previous research, we argue that such assumption might be hazardous, especially for complex tasks and small demonstrations datasets (Zare et al., 2023; Ross et al., 2011; Kelly et al., 2019; Malato et al., 2022). Whenever the optimality assumption is not satisfied, π_θ might learn to follow a suboptimal policy and, as such, get stuck in a local minimum. In Figure 2 we show an example of this behaviour from our preliminary experiments for the present study.

5. Experiments

We use vanilla cDQL as main comparison for our experiments, and compare them to our improved agents. Additionally, we include HER, QDagger, LOGO and AWAC as additional baselines. As some of the agent we tested require pre-training, we train a simple *Behavioral Cloning* (BC) (Torabi et al., 2018) baseline and use it as expert policy. Each BC agent is trained on the same dataset that we leverage with our method. To select the best possible expert policy, we extensively tested each BC policy during training and retained only the one with the highest mean reward. Our source code for the experiment is available at [hidden information][1].

[1]The link is temporarily removed to preserve anonimity of the submission

We demonstrate our approach a total of five environments from the Miniworld (Chevalier-Boisvert et al., 2023) benchmark. Specifically, we test the agents on three navigation environments, *OneRoom*, *FourRooms*, and *MazeS3*; additionally, we include a constrained navigation environment, *Sidewalk*, and survival-based task named *CollectHealth* from the same suite. These environments are partially observable and feature 80×60 RGB images as input, which we resize to 64×64 for convenience; additionally, the reward is sparse and delayed, being observed at the end of an episode *only if the agent is successful*. The action space is discrete.

Data collection For each environment we manually collected approximately 5 minutes of experience, amounting to 10 trajectories for more complex tasks (e.g. *MazeS3*) and 20 trajectories for easier ones, such as *OneRoom*. On average, each trajectory lasts around 150 timesteps for complex tasks and 75 for quicker ones, hence an agent has approximately 1500 transitions per task at its disposal.

Network architectures Our DQN implementation is taken from CleanRL (Huang et al., 2021). All other models are built on top of the same code base, preserving the original as much as possible and implementing only the algorithm-specific changes to it. For LOGO, we re-implemented a basic version of TRPO and edited it, following the source code provided by the authors of the original paper. All our DQN-derived policies are MLPs with two hidden layers, of 256 units each. For TRPO, we use MLPs with two hidden layers, equipped with 512 units each.

To process visual inputs, we train a beta-variational autoencoder (β-VAE) (Kingma & Welling, 2022; Higgins et al., 2017) neural network with four convolutional layers, followed by a flattening layer and a dense layer to project the flattened features into the desired latent space. The network takes a single 64×64 RGB image as input and outputs a latent of size 128. Each β-VAE is trained to simply reconstruct the input image, with no conditioning on action selection. We pre-train an encoder for each environment using a dataset of 400 trajectories collected by a random policy. After training, we detach the decoder and only use the encoder as features extractor. All tested agents share the same features extractor. A list of hyperparameters is available in Appendix A.

6. Results

The results of our experiments are shown in Figure 3. For each agent, we report the value of the reward on the y-axis and the number of timesteps on the x-axis. Our results are also publicly available on Weight&Biases (Biewald et al.)

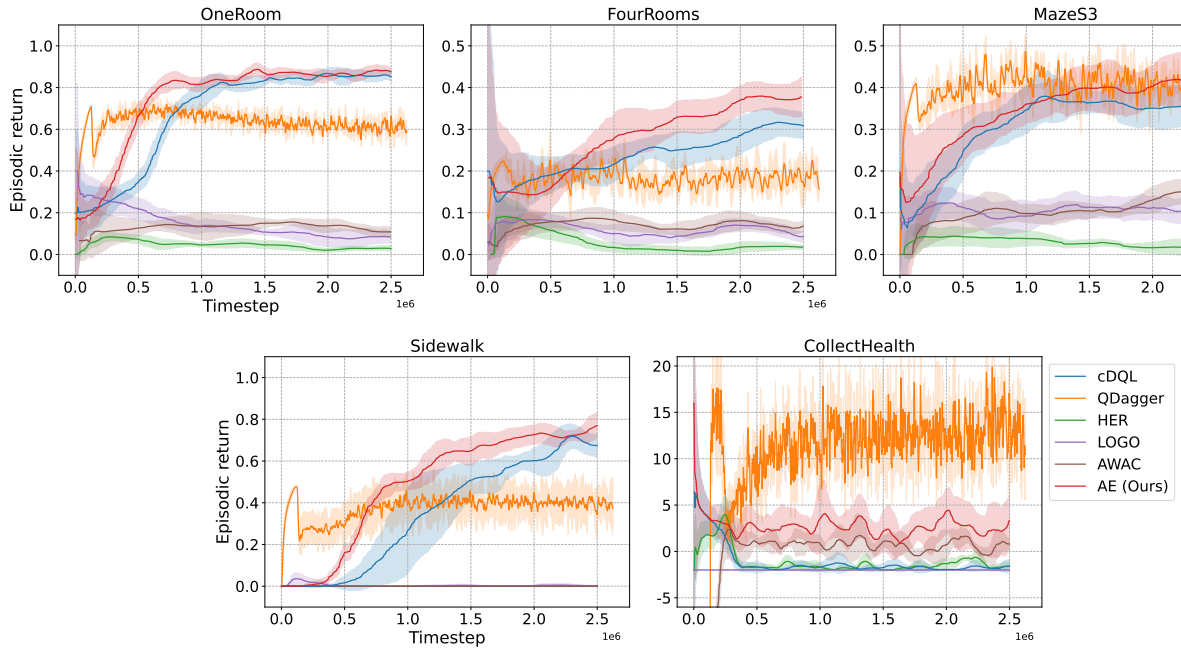

Figure 3. Comparison between our agent (red) compared to five baselines, cDQL (blue), QDagger (orange), HER (green), LOGO (purple), and AWAC (brown). Agents are trained for 2.5M timesteps. Each training is repeated five times on different seeds.

at [hidden information][2], along with additional relevant metrics and media. Additionally, we report a subset of numerical results in Table 2, highlighting the change in mean reward as train progresses. The full version of these results is available in Appendix B.

Our method improves sample efficiency of cDQL in all tasks. This is especially visible in *OneRoom*, *Sidewalk* and *CollectHealth*. Notably, vanilla cDQL completely fails in the latter task, while our agent can in some cases solve it. Similarly, agent trained with QDagger and AWAC learns to successfully collect some medkits. We point out that the environment is quite difficult for all tested agents, as it requires to approach medkits and then actively gathering them by pressing a key, while the medkit is not in sight. This is a design feature of the environment itself.

Numerically, in *OneRoom* our agent reaches an average reward of 0.8 after around 750k timesteps, while the cDQL baseline only reaches the same performance after roughly 1.2M steps. That is, speeding up convergence of 37.5%. No other baseline method converges to that value of the reward. Similarly, in *Sidewalk* our agent reaches 0.6 average reward after around 1.2M, while vanilla cDQL reaches the same performance at 1.8M, that is, using 33.3% more transitions. Notably, cDQL with Adversarial Estimates converges at an average reward of 0.738 ± 0.062, while vanilla cDQL only reaches 0.663 ± 0.215. This fact follows from our claim that our method does not bound a policy to follow the expert, rather encourages to improve over it. We highlight that HER, LOGO and AWAC completely fail the task, while QDagger converges to a mean average of 0.373 ± 0.018. Notably, in both tasks QDagger obtains a higher mean reward than our method in the early stages of training as a result of pre-training. Then, QDagger clearly remains trapped in a local minimum. Contrary to the findings of the authors (Agarwal et al., 2022), in our experiments using a suboptimal BC agent to pre-train QDagger had an impact on its performance. We attribute this mismatch to the difficulty of solving an image-based, partially observable environment: as the information available to an agent is very limited, QDagger might require a near-optimal expert.

AWAC and HER completely fail *Sidewalk*. Despite showing some promise at the beginning of training, also LOGO is unable to leverage the expert data for this task. Additionally, all three methods achieve only faint results in *OneRoom* (mean reward around 0.1). This last result is unexpected, especially after the promising starts that all agents showed.

Despite our best efforts, our results differ significantly from the ones reported in the original papers. We believe that this gap is to be attributed to the inherent difficulty of the tasks in Miniworld. In particular, the observation carries a small amount of information. Additionally, the reward is observed only on the last timestep of an episode, and only in case of success. As such, it is quite common to observe no reward

[2]The link is temporarily removed to preserve anonimity of the submission

Table 2. Numerical results for our training runs on the two most representative environments, *OneRoom* and *Sidewalk*. All agents have been trained for five times on five different seeds. For each agent, we report the mean reward and standard deviation obtained during training every 500k timesteps. Full results are available in Appendix B.

Environment	Algorithm	Reward@500k	Reward@1M	Reward@1.5M	Reward@2M	Reward@2.5M
OneRoom	cDQL	0.349 ± 0.044	0.796 ± 0.061	0.845 ± 0.022	0.867 ± 0.028	0.851 ± 0.022
	HER	0.067 ± 0.024	0.045 ± 0.010	0.046 ± 0.019	0.020 ± 0.010	0.029 ± 0.014
	QDagger	$\mathbf{0.679 \pm 0.032}$	0.662 ± 0.014	0.608 ± 0.027	0.606 ± 0.033	0.591 ± 0.026
	LOGO	0.209 ± 0.049	0.137 ± 0.032	0.106 ± 0.016	0.078 ± 0.040	0.087 ± 0.029
	AWAC	0.129 ± 0.032	0.135 ± 0.066	0.149 ± 0.021	0.137 ± 0.032	0.109 ± 0.027
	AE (Ours)	0.669 ± 0.062	$\mathbf{0.817 \pm 0.031}$	$\mathbf{0.873 \pm 0.029}$	$\mathbf{0.853 \pm 0.029}$	$\mathbf{0.876 \pm 0.018}$
Sidewalk	cDQL	0.025 ± 0.047	0.301 ± 0.204	0.520 ± 0.074	0.601 ± 0.063	0.673 ± 0.055
	HER	0.000 ± 0.000	0.000 ± 0.000	0.000 ± 0.000	0.000 ± 0.000	0.000 ± 0.000
	QDagger	$\mathbf{0.283 \pm 0.099}$	0.393 ± 0.104	0.408 ± 0.088	0.438 ± 0.047	0.373 ± 0.104
	LOGO	0.003 ± 0.004	0.000 ± 0.000	0.004 ± 0.005	0.002 ± 0.004	0.002 ± 0.003
	AWAC	0.000 ± 0.000	0.000 ± 0.000	0.000 ± 0.000	0.000 ± 0.000	0.000 ± 0.000
	AE (Ours)	0.148 ± 0.040	$\mathbf{0.501 \pm 0.038}$	$\mathbf{0.646 \pm 0.066}$	$\mathbf{0.727 \pm 0.046}$	$\mathbf{0.769 \pm 0.060}$

in the early stages of training, hence preventing learning or severely limiting the capabilities of an agent.

We highlight the smaller improvement of our method on *MazeS3* and in *FourRooms* over the standard cDQL. In the first case, using Adversarial Estimates allows cDQL to converge to a higher reward, 0.381 ± 0.051, in contrast with the baseline that tops at 0.357 ± 0.044. Notably, our method reaches the same performance as the baseline in 860k timesteps, hence using 65.6% less frames than regular cDQL. In *FourRooms*, using Adversarial Estimates improves over the baseline (cDQL 0.308 ± 0.246, AE 0.377 ± 0.048), and matches the baseline best reward after only 975k timesteps, just above a third of the time. Like other tasks, QDagger is the only direct competitor of our approach. Still, while it shows better behavior in the early stages of training, also on this task QDagger converges to a local minimum. Similarly to the other tasks, AWAC, LOGO and HER are unable to complete *FourRooms* reliably, reaching a maximum performance of 0.068 ± 0.012, 0.044 ± 0.013 and 0.018 ± 0.005 respectively. However, we notice that all compared agents converge to a low reward. We explain this shortcoming with the difficulty of the environments: in particular, learning to navigate in complex environments with very sparse rewards represents a considerable challenge, especially with a relatively tight time budget. As such, we believe that relaxing these constraints might lead to an improvement in performance.

7. Conclusions

We have presented *Adversarial Estimates*, a new approach to improve the sample efficiency of a DRL agent based on game theory and search. Our approach improves over the other approaches, as it is more easily and widely applicable. Moreover, its requirements are very loose, it requires no pre-training, and its effects are visible with as low as five minutes of collected experience.

Limitations Adversarial Estimates is far from being perfect. While being useful, it can be applied only on tasks where previous experience can be collected. Also, while not explicitly requiring optimal data, using very low quality data, such as a dataset gathered from a random policy, would likely result in a significant loss in performance. Finally, our approach is based on over-estimating the Q-values of the expert. As such, whenever such estimation fails, our approach will fail as well.

Future work In our work, we have studied Adversarial Estimates as a way to kickstart training in off-policy DRL algorithms. However, we hypothesize that our formulation could be extended to on-policy methods as well. In particular, actor-critic on-policy algorithms such as TRPO (Schulman et al., 2017a) and *Proximal policy Optimization* (PPO) (Schulman et al., 2017b) rely on a value function critic providing a feedback $V(s)$, rather than an action-value estimate $Q(s, a)$. We believe that introducing an action-value critic could be key to make our approach applicable to such algorithms.

Another interesting research direction would include combining our approach with other approaches. For instance, it would be interesting to combine our approach with QDagger, perhaps leveraging our search-based policy as teacher, hence improving the pre-training phase.

Impact Statement

This paper presents a new approach for improving sample efficiency in Reinforcement Learning (RL). We believe that our contributions could pose another step towards making RL more applicable in real world scenarios. In particular, improving sample efficiency with the use of minimal data leads to better and faster convergence, hence lowering the costs of such applications and increasing their appeal. Simultaneously, using small datasets reduces the cost of gathering examples, leading to more contained time and monetary budgets.

References

Agarwal, R., Schwarzer, M., Castro, P. S., Courville, A., and Bellemare, M. G. Reincarnating reinforcement learning: Reusing prior computation to accelerate progress, 2022. URL https://arxiv.org/abs/2206.01626.

Andrychowicz, M., Wolski, F., Ray, A., Schneider, J., Fong, R., Welinder, P., McGrew, B., Tobin, J., Abbeel, P., and Zaremba, W. Hindsight experience replay, 2018. URL https://arxiv.org/abs/1707.01495.

Bellemare, M. G., Srinivasan, S., Ostrovski, G., Schaul, T., Saxton, D., and Munos, R. Unifying count-based exploration and intrinsic motivation, 2016. URL https://arxiv.org/abs/1606.01868.

Biewald, L., Pelt, C. V., and Lewis, S. Weight & biases homepage. URL https://wandb.ai/site/papers/.

Chevalier-Boisvert, M., Dai, B., Towers, M., de Lazcano, R., Willems, L., Lahlou, S., Pal, S., Castro, P. S., and Terry, J. Minigrid & miniworld: Modular & customizable reinforcement learning environments for goal-oriented tasks, 2023. URL https://arxiv.org/abs/2306.13831.

Fujimoto, S., van Hoof, H., and Meger, D. Addressing function approximation error in actor-critic methods, 2018. URL https://arxiv.org/abs/1802.09477.

Haarnoja, T., Zhou, A., Abbeel, P., and Levine, S. Soft actor-critic: Off-policy maximum entropy deep reinforcement learning with a stochastic actor, 2018. URL https://arxiv.org/abs/1801.01290.

Hester, T., Vecerik, M., Pietquin, O., Lanctot, M., Schaul, T., Piot, B., Horgan, D., Quan, J., Sendonaris, A., Dulac-Arnold, G., Osband, I., Agapiou, J., Leibo, J. Z., and Gruslys, A. Deep q-learning from demonstrations, 2017. URL https://arxiv.org/abs/1704.03732.

Higgins, I., Matthey, L., Pal, A., Burgess, C., Glorot, X., Botvinick, M., Mohamed, S., and Lerchner, A. beta-VAE: Learning basic visual concepts with a constrained variational framework. In *International Conference on Learning Representations*, 2017. URL https://openreview.net/forum?id=Sy2fzU9gl.

Huang, S., Dossa, R. F. J., Ye, C., and Braga, J. Cleanrl: High-quality single-file implementations of deep reinforcement learning algorithms, 2021. URL https://arxiv.org/abs/2111.08819.

Kelly, M., Sidrane, C., Driggs-Campbell, K., and Kochenderfer, M. J. Hg-dagger: Interactive imitation learning with human experts, 2019. URL https://arxiv.org/abs/1810.02890.

Kingma, D. P. and Welling, M. Auto-encoding variational bayes, 2022. URL https://arxiv.org/abs/1312.6114.

Lillicrap, T. P., Hunt, J. J., Pritzel, A., Heess, N., Erez, T., Tassa, Y., Silver, D., and Wierstra, D. Continuous control with deep reinforcement learning, 2019. URL https://arxiv.org/abs/1509.02971.

Malato, F. and Hautamäki, V. Online adaptation for enhancing imitation learning policies. In *2024 IEEE Conference on Games (CoG)*, pp. 1–8, 2024. doi: 10.1109/CoG60054.2024.10645565.

Malato, F., Jehkonen, J., and Hautamäki, V. Improving behavioural cloning with human-driven dynamic dataset augmentation, 2022. URL https://arxiv.org/abs/2201.07719.

Mnih, V., Kavukcuoglu, K., Silver, D., Rusu, A. A., Veness, J., Bellemare, M. G., Graves, A., Riedmiller, M., Fidjeland, A. K., Ostrovski, G., Petersen, S., Beattie, C., Sadik, A., Antonoglou, I., King, H., Kumaran, D., Wierstra, D., Legg, S., and Hassabis, D. Human-level control through deep reinforcement learning. *Nature*, 518 (7540):529–533, February 2015. ISSN 00280836. URL http://dx.doi.org/10.1038/nature14236.

Nair, A., Gupta, A., Dalal, M., and Levine, S. Awac: Accelerating online reinforcement learning with offline datasets, 2021. URL https://arxiv.org/abs/2006.09359.

Rengarajan, D., Vaidya, G., Sarvesh, A., Kalathil, D., and Shakkottai, S. Reinforcement learning with sparse rewards using guidance from offline demonstration, 2022. URL https://arxiv.org/abs/2202.04628.

Ross, S., Gordon, G. J., and Bagnell, J. A. A reduction of imitation learning and structured prediction to no-regret online learning, 2011. URL https://arxiv.org/abs/1011.0686.

Schmitt, S., Hudson, J. J., Zidek, A., Osindero, S., Doersch, C., Czarnecki, W. M., Leibo, J. Z., Kuttler, H., Zisserman, A., Simonyan, K., and Eslami, S. M. A. Kickstarting deep reinforcement learning, 2018. URL https://arxiv.org/abs/1803.03835.

Schulman, J., Levine, S., Moritz, P., Jordan, M. I., and Abbeel, P. Trust region policy optimization, 2017a. URL https://arxiv.org/abs/1502.05477.

Schulman, J., Wolski, F., Dhariwal, P., Radford, A., and Klimov, O. Proximal policy optimization algorithms, 2017b. URL https://arxiv.org/abs/1707.06347.

Shakya, A. K., Pillai, G., and Chakrabarty, S. Reinforcement learning algorithms: A brief survey. *Expert Systems with Applications*, 231:120495, 2023. ISSN 0957-4174. doi: https://doi.org/10.1016/j.eswa.2023.120495. URL https://www.sciencedirect.com/science/article/pii/S0957417423009971.

Sutton, R. S. and Barto, A. G. *Reinforcement Learning: An Introduction*. The MIT Press, second edition, 2018. URL http://incompleteideas.net/book/the-book-2nd.html.

Torabi, F., Warnell, G., and Stone, P. Behavioral cloning from observation, 2018. URL https://arxiv.org/abs/1805.01954.

Vecerik, M., Hester, T., Scholz, J., Wang, F., Pietquin, O., Piot, B., Heess, N., Rothörl, T., Lampe, T., and Riedmiller, M. Leveraging demonstrations for deep reinforcement learning on robotics problems with sparse rewards, 2018. URL https://arxiv.org/abs/1707.08817.

Zare, M., Kebria, P. M., Khosravi, A., and Nahavandi, S. A survey of imitation learning: Algorithms, recent developments, and challenges, 2023. URL https://arxiv.org/abs/2309.02473.

A. Hyperparameters

Table 3. Hyperparameters used for training the β-VAE.

Name	Value
latent size	128
channels	$[3, 32, 64, 128]$
kernel size	$[4, 4, 4, 4]$
stride	$[2, 2, 2, 2]$
learning rate	3×10^{-4}
batch size	128
epochs	30
temperature	$0.0 \rightarrow 5 \times 10^{-8}$
temp. increase	$0.1 * \text{epochs} \rightarrow 0.9 * \text{epochs}$

In this section, we list the hyperparameters we have used to train our models, to ensure reproducibility. More specifically, in Tables 3 and 4 we report the hyperparameters we used to train the VAE encoders and the common hyperparameters of cDQL, respectively. These parameters are shared across all algorithms. Additionally, in each subsection we disclose the algorithm-specific parameters that we have used.

Table 4. Hyperparameters used for training all instances of cDQL.

Name	Value
learning rate	1×10^{-4}
γ	0.99
τ	1.0
buffer size	250000
batch size	32
ϵ	$1.0 \rightarrow 0.05$
exploration fraction	0.1
target train frequency	1000
train frequency	4

For cDQL, we retain most of the values used in the CleanRL code. Due to memory constraints, we resize the buffer size to a quarter of the original size. Consistently, we reduce the timesteps budget for our agents down to a quarter of the original size. We justify this choice by highlighting that all the agents have converged after 2.5M steps. Additionally, by equally scaling down these two parameters, we ensure that the buffer size is completely filled by the time the end of exploration occurs, hence ensuring plenty of time for an agent to explore the state space extensively.

A.1. HER

HER does not have specific hyperparameters. However, we tuned the number of subgoals to be imposed for each batch, and found the best results for $n = 16$. As such, after the regular sampling from the replay buffer, we sample an additional 16 transitions and impose a reward of 1.

A.2. LOGO

Table 5. A list of hyperparameters used for LOGO.

Name	Value
# rollouts	10
max KL	0.01
batch size (discriminator)	256
learning rate	3×10^{-4}

In the partial observability case, LOGO uses an additional discriminator network to discern between the state-actions pairs (s, a) generated by the policy and the ones generated by the expert. In our experiments, we train the discriminator using the same hyperparameters as the original code base, that is, a batch size of 256 and a learning rate of 3×10^{-4}. The other hyperparameters listed in Table 5, # rollouts and max KL, refer to the number of rollouts to gather before an update and the size of the trust region, respectively.

A.3. QDagger

Table 6. List of hyperparameters used in our QDagger implementation and their relative values.

Name	Value
teacher steps	125000
offline steps	125000
teacher evaluation episodes	10
τ	1.0
λ	1.0

QDagger uses an additional pre-training phase on a replay buffer of transitions sampled by the expert policy. In our experiments, we train a simple BC policy using our dataset and use it to gather 125k transitions. Then, we pre-train the agent on the BC-collected dataset for an additional 125k steps. Finally, the agent is trained online with an additional distillation term balanced with λ. The hyperparameters are summarized in Table 6.

A.4. AWAC

Table 7. Hyperparameters used for training cDQL using the AWAC update.

Name	Value
offline steps	100000
offline eval episodes	10
λ	0.3

AWAC features a pre-training phase. We report the specific hyperparameters in Table 7. In our experiments, we pre-train the agent for 100k steps and keep track of its performance by testing it on 10 evaluation episodes every 1000 forward passes. The offline and online phases use the same closed-form update derived by the authors. Additionally, a scaling term $\lambda = 0.3$ balances the effect of the update.

A.5. Adversarial Estimates

Our method does not use additional hyperparameters w.r.t. to the cDQL baseline. One exception is an optional scaling factor $\lambda \in [0, 1]$ to balance the effect of the adversarial estimates on the total loss. In our experiments, we leave $\lambda = 1.0$.

B. Full training results

Table 8 summarizes the results of our experiments as reported in Section 6 (Figure 3). As discussed in the main paper, adversarial estimates improves sample efficiency **and** performance on every task, with respect to the cDQL baseline. Notably, QDagger improves over our method in *CollectHealth*. Additionally, its pre-training phase allows it to reach higher mean reward at 500k steps on every task. Despite this, Adversarial Estimates improves in the later stages, possibly due to the expert optimality assumption of the BC agent. By following it during pre-training, QDagger converges to a local minimum in three tasks (*OneRoom*, *FourRooms* and *Sidewalk*), hence demonstrating the partial disadvantage of relying on previously trained agents for policy training.

Table 8. Full version of Table 2, shown in Section 6.

Environment	Algorithm	Reward@500k	Reward@1M	Reward@1.5M	Reward@2M	Reward@2.5M
OneRoom	cDQL	0.349 ± 0.044	0.796 ± 0.061	0.845 ± 0.022	0.867 ± 0.028	0.851 ± 0.022
	HER	0.067 ± 0.024	0.045 ± 0.010	0.046 ± 0.019	0.020 ± 0.010	0.029 ± 0.014
	QDagger	$\mathbf{0.679 \pm 0.032}$	0.662 ± 0.014	0.608 ± 0.027	0.606 ± 0.033	0.591 ± 0.026
	LOGO	0.209 ± 0.049	0.137 ± 0.032	0.106 ± 0.016	0.078 ± 0.040	0.087 ± 0.029
	AWAC	0.129 ± 0.032	0.135 ± 0.066	0.149 ± 0.021	0.137 ± 0.032	0.109 ± 0.027
	AE (Ours)	0.669 ± 0.062	$\mathbf{0.817 \pm 0.031}$	$\mathbf{0.873 \pm 0.029}$	$\mathbf{0.853 \pm 0.029}$	$\mathbf{0.876 \pm 0.018}$
FourRooms	cDQL	0.193 ± 0.042	0.219 ± 0.040	0.250 ± 0.042	0.282 ± 0.046	0.308 ± 0.031
	HER	0.061 ± 0.024	0.017 ± 0.011	0.011 ± 0.010	0.013 ± 0.013	0.018 ± 0.005
	QDagger	$\mathbf{0.221 \pm 0.059}$	0.218 ± 0.029	0.171 ± 0.030	0.169 ± 0.023	0.156 ± 0.021
	LOGO	0.080 ± 0.014	0.051 ± 0.027	0.041 ± 0.013	0.069 ± 0.014	0.044 ± 0.013
	AWAC	0.077 ± 0.022	0.084 ± 0.024	0.061 ± 0.018	0.082 ± 0.021	0.067 ± 0.012
	AE (Ours)	0.150 ± 0.056	$\mathbf{0.271 \pm 0.052}$	$\mathbf{0.324 \pm 0.038}$	$\mathbf{0.360 \pm 0.035}$	$\mathbf{0.377 \pm 0.048}$
Sidewalk	cDQL	0.025 ± 0.047	0.301 ± 0.204	0.520 ± 0.074	0.601 ± 0.063	0.673 ± 0.055
	HER	0.000 ± 0.000	0.000 ± 0.000	0.000 ± 0.000	0.000 ± 0.000	0.000 ± 0.000
	QDagger	$\mathbf{0.283 \pm 0.099}$	0.393 ± 0.104	0.408 ± 0.088	0.438 ± 0.047	0.373 ± 0.104
	LOGO	0.003 ± 0.004	0.000 ± 0.000	0.004 ± 0.005	0.002 ± 0.004	0.002 ± 0.003
	AWAC	0.000 ± 0.000	0.000 ± 0.000	0.000 ± 0.000	0.000 ± 0.000	0.000 ± 0.000
	AE (Ours)	0.148 ± 0.040	$\mathbf{0.501 \pm 0.038}$	$\mathbf{0.646 \pm 0.066}$	$\mathbf{0.727 \pm 0.046}$	$\mathbf{0.769 \pm 0.060}$
CollectHealth	cDQL	-1.676 ± 0.618	-1.749 ± 0.392	-1.784 ± 0.362	-1.954 ± 0.075	-1.612 ± 0.683
	HER	-1.624 ± 0.330	-1.688 ± 0.441	-1.985 ± 0.017	-1.333 ± 0.492	-1.580 ± 0.553
	QDagger	$\mathbf{9.466 \pm 1.373}$	$\mathbf{10.025 \pm 2.637}$	$\mathbf{10.827 \pm 2.358}$	$\mathbf{9.464 \pm 2.023}$	$\mathbf{10.616 \pm 4.139}$
	LOGO	-2.000 ± 0.000	-2.000 ± 0.000	-2.000 ± 0.000	-2.000 ± 0.000	-2.000 ± 0.000
	AWAC	1.133 ± 0.530	0.952 ± 0.809	1.063 ± 0.695	1.226 ± 1.156	0.801 ± 0.698
	AE (Ours)	2.400 ± 1.583	3.839 ± 3.780	1.708 ± 1.912	4.530 ± 2.540	3.309 ± 2.786
MazeS3	cDQL	0.253 ± 0.059	0.357 ± 0.058	0.364 ± 0.027	0.351 ± 0.044	0.357 ± 0.044
	HER	0.040 ± 0.022	0.035 ± 0.015	0.029 ± 0.008	0.017 ± 0.015	0.015 ± 0.013
	QDagger	$\mathbf{0.388 \pm 0.044}$	$\mathbf{0.452 \pm 0.035}$	$\mathbf{0.435 \pm 0.029}$	0.394 ± 0.026	0.359 ± 0.034
	LOGO	0.120 ± 0.034	0.093 ± 0.040	0.112 ± 0.025	0.112 ± 0.028	0.108 ± 0.027
	AWAC	0.082 ± 0.038	0.098 ± 0.022	0.104 ± 0.016	0.134 ± 0.033	0.137 ± 0.031
	AE (Ours)	0.301 ± 0.058	0.363 ± 0.044	0.397 ± 0.057	$\mathbf{0.406 \pm 0.055}$	$\mathbf{0.381 \pm 0.051}$